XLVI CILAMCE
VITÓRIA - ES - BRAZIL - 2025
XLVI IBERO-LATIN AMERICAN CONGRESS ON COMPUTATIONAL METHODS IN ENGINEERING

NUMERICAL ANALYSIS OF LOCAL-GLOBAL BUCKLING INTERACTION IN LAMINATED COMPOSITE CHANNEL COLUMNS

Pedro Sanderson Bastos Barros[1], Carlos Hiago Ramos Monteiro[2], Luiz Antônio Taumaturgo Mororó[3], Marcelo Silva Medeiros Júnior[2], Evandro Parente Junior[2]

[1]*Instituto Federal do Ceará – Campus Itapipoca*
Av. da Universidade, 102, 62500-000, Itapipoca, Ceará, Brasil
pedro.barros@ifce.edu.br
[2]*Departmento de Engenharia Estrutural e Construção Civil, Universidade Federal do Ceará*
Campus do Pici, Bloco 733, 60440-900, Fortaleza, Ceará, Brasil
hiagomonteiro@alu.ufc.br, *marcelomedeiros@ufc.br*, *evandro@ufc.br*
[3]*Instituto Federal do Ceará – Campus Fortaleza*
Av. Treze de Maio, 60040-531, Fortaleza, Ceará, Brasil
luiz.mororo@ifce.edu.br

Abstract. The study of buckling of thin-walled structures is essential to ensure safety, efficiency, and economic feasibility in structural design, as these systems are particularly prone to instability phenomena. Channels, widely used in structural applications, can exhibit various buckling modes: local (plate-type), global (flexural and flexural-torsional), or through interactions between these modes. Accurate design must account for such interactions to ensure sufficient structural capacity, as understanding these mechanisms is crucial for reliably predicting the behavior of compressed columns and preventing premature failure. These stability problems become even more complex when advanced materials, such as fiber-reinforced composites, are employed. These materials have attracted significant attention due to their high specific strength, corrosion resistance, and tailorability. In thin-walled members, fiber-reinforced composites enable the optimization of mechanical performance through controlled ply orientations and stacking sequences. Nonetheless, their anisotropic behavior introduces significant complexity in accurately predicting structural buckling responses. Therefore, this work aims to develop a numerical model using the Finite Element Method to investigate the interaction between local and global buckling in simply supported fiber-reinforced composite channel columns under axial compression, and to assess the influence of initial geometric imperfections on the load-carrying capacity of these structural elements.

Keywords: Laminated composites; Channel columns; Post-buckling behavior; Imperfection analysis.

1 Introduction

Buckling is a major concern in the design of thin-walled structures, since they tend to be very slender, and failure can occur with stresses much lower than the material's strength. Thin-walled channels, widely used in structural applications, can exhibit local (plate-type) or global (flexural and flexural-torsional) as main buckling modes. Furthermore, these modes can interact reducing the load-carrying capacity.

Wang et al. [1] investigated experimentally and numerically the buckling behavior of cold-formed steel (CFS) built-up closed section columns (formed by a lipped channel and a channel spliced together by connecting the flanges utilizing self-drilling screws) affected by local-global (L-G) interaction for estimating the load carrying capacity of the section. The accuracy of several design specifications for predicting this load carrying capacity was also evaluated by the authors. Dinis et al. [2] presented results on the behavior and Direct Strength Method (DSM) -based design of fixed-ended CFS channel and lipped channel columns that exhibit flexural-torsional (F_MT)

buckling – i.e., flexure about the major axis coupled with torsion – and flexural (F_m) buckling about the minor axis. The interaction between these two global modes characterizes the global-global (G-G) buckling interaction studied. The study investigates both the buckling and post-buckling response, with emphasis on identifying the most detrimental initial geometric imperfection. Based on the results, the authors propose a modification in the DSM to better capture G-G interaction effects. Cerqueira et al. [3] extends the investigation presented in [2] by analyzing fixed-ended CFS columns with a wider range of cross-section shapes, all monosymmetric with respect to the major axis.

A laminated fiber-reinforced composite is a type of composite material made by stacking multiple layers (layup) of fiber-reinforced material. Each layer consists of fibers (such as glass, carbon, or aramid) embedded in a polymeric matrix. The fibers in each layer can be oriented in different directions to optimize one or more mechanical properties of the material, like strength or stiffness [4, 5]. These materials have attracted significant attention due to their high specific strength, corrosion resistance, and tailorability.

Czapski and Lunt [6] investigated the influence of manufacturing methods on the buckling and post-buckling behavior of carbon fiber-reinforced polymer (CFRP) channel columns composed of symmetric angle-ply laminates. Two fabrication techniques were compared: conventional channel lamination and cutting from a square tube. The latter proved more material-efficient and offered higher buckling resistance. Finite element models showed that residual stresses significantly influenced the performance of the cut-from-square specimens, underscoring the importance of manufacturing-induced effects in the design of laminated channels. Debski et al. [7-10] present experimental results for the local buckling of laminated channel columns and other column profiles with different layups, and compare them with results obtained using shell finite element models. D'Aguiar and Parente [11] proposed an approximate methodology for evaluating the local buckling load of laminated columns with channel sections and studied the post-critical behavior of imperfect columns using shell finite elements.

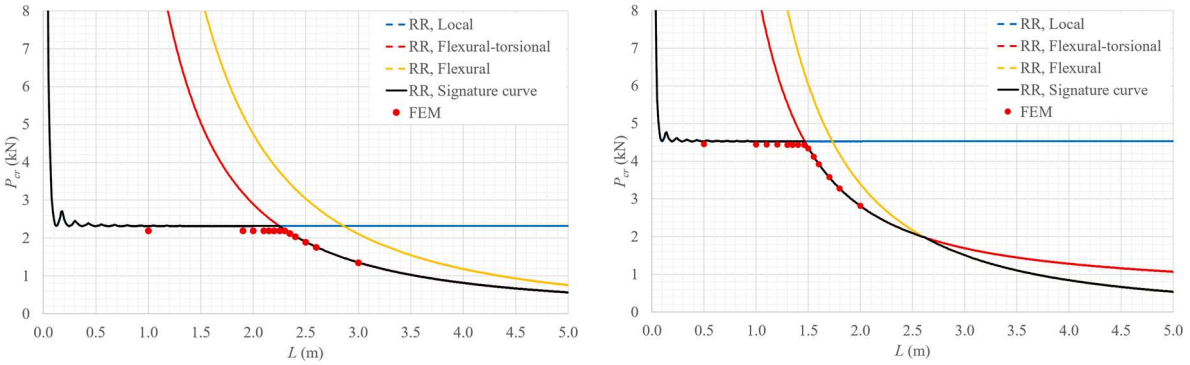
This work aims to develop a numerical model using the Finite Element Method (FEM) to investigate the interaction between local and global buckling in simply supported fiber-reinforced composite channel columns under axial compression and to assess the influence of initial geometric imperfections on the load-carrying capacity of these structural elements.

2 Methodology

This item is dedicated to outlining the main features of the procedure adopted in this work. The next paragraphs present the columns geometrical parameters chosen for the proposed study, the mechanical properties of the composite material, the adopted layups, the finite element model of the columns used in this paper, and how the initial geometric imperfection were considered.

The cross-section dimensions of the channel columns are web height b_w = 80 mm, flange width b_f = 40 mm, and total thickness h = 1.048 mm. The composite Hexcel's HexPly M12 carbon-epoxy was considered in this work. The mechanical properties of this material are E_1 = 130.71 GPa, E_2 = 6.36 GPa, G_{12} = 4.18 GPa, and ν_{12} = 0.32 [7]. Two different layups were considered, and they are named L1 $[0°/90°/0°/90°]_S$ and L2 $[45°/-45°/90°/0°]_S$.

To determine the length of the columns in the transition of the local buckling mode to the flexural-torsional, the signature curves for each layup are examined. For this work, these signature curves were obtained by using the Classical Lamination Theory [4, 5] and a Rayleigh-Ritz (RR) approximation combined with (*a*) the Classical Plate Theory to determine the local critical loads [5, 12], and (*b*) with Kollar and Pluszik theories [13, 14] for thin-walled beams to determine the geometrical properties of the cross-section and the global buckling loads [15, 16]. The signature curves for the cross-section adopted and for each layup is presented in Figure 1. In addition, Table 1 presents the buckling modes transition length, the critical loads obtained, and the ratio R between the local and flexural-torsional buckling loads ($R = P_{cr,L} / P_{cr,FT}$) for each layup. For the next steps, the considered buckling modes transition lengths for the columns with layups L1 and L2 are, respectively, 2300 mm and 1460 mm.



(a) Layup L1. (b) Layup L2.

Figure 1. Signature curves.

Table 1. Buckling loads and transition lengths.

Layup	Rayleigh-Ritz				FEM				Differences (%)	
	L (m)	$P_{cr,L}$ (kN)	$P_{cr,FT}$ (kN)	R	L (m)	$P_{cr,L}$ (kN)	$P_{cr,FT}$ (kN)	R	$P_{cr,L}$	$P_{cr,FT}$
L1	2.300	2.320	2.221	1.045	2.300	2.193	2.202	0.996	5.80%	0.86%
L2	1.460	4.533	4.549	0.996	1.460	4.436	4.530	0.979	2.19%	0.42%

To refine the transition length estimates with greater accuracy, the critical buckling loads of the columns were determined using FEM [17, 18] through the commercial software ABAQUS [19]. The columns were modeled with simply supported boundary conditions, and a uniform compressive load was applied. The finite element mesh employed S8R quadratic shell elements with reduced integration and six degrees of freedom per node, using a uniform discretization of 10 mm × 10 mm. The post-buckling equilibrium paths, incorporating local-global mode interaction, were obtained through geometrically nonlinear analyses using the arc-length method to trace the behavior of the columns.

In the nonlinear analysis of the columns, the imperfect geometry of the columns can be modeled as a linear combination of its buckling modes ($\boldsymbol{\varphi}_i$):

$$\mathbf{x}_{imp} = \mathbf{x}_{perf} + \sum \Delta_i \boldsymbol{\varphi}_i \tag{1}$$

where $\mathbf{x}_{imp}$ and $\mathbf{x}_{perf}$ are the coordinates of the points defining the geometry in the imperfect and perfect configurations, respectively, and Δ_i is the imperfection amplitude associated with the normalized buckling mode $\boldsymbol{\varphi}_i$.

To assess the influence of initial imperfections in the geometrically nonlinear analyses performed for the transition length between local and flexural-torsional buckling modes of the columns, the imperfection amplitude Δ_i is defined as $\Delta_i = \alpha\, \Delta_{i,max}$ (with $i = L$ or FT, for the local or flexural-torsional buckling mode, respectively), such that Eq. (1) can be rewritten as follows:

$$\mathbf{x}_{imp} = \mathbf{x}_{perf} + \Delta_L\, \boldsymbol{\varphi}_L + \Delta_{FT}\, \boldsymbol{\varphi}_{FT} = \mathbf{x}_{perf} + \alpha_L\, \Delta_{L,max}\, \boldsymbol{\varphi}_L + \alpha_{FT}\, \Delta_{FT,max}\, \boldsymbol{\varphi}_{FT} \tag{2}$$

being $\Delta_{L,max} = h/10$, and $\Delta_{FT,max} = L/1000$. Table 2 shows the combinations of imperfections evaluated in this paper.

Table 2. Imperfection combinations analysed.

Imperfection Combination	α_L	α_{FT}	Layup L1		Layup L2	
			Δ_L	Δ_{FT}	Δ_L	Δ_{FT}
C1	0.00	1.00	0.0000	2.3000	0.0000	1.4600
C2	0.50	0.50	0.0524	1.1500	0.0524	0.7300
C3	1.00	0.00	0.1048	0.0000	0.1048	0.0000

Table 3. Initial geometric imperfections analysed for pure buckling modes.

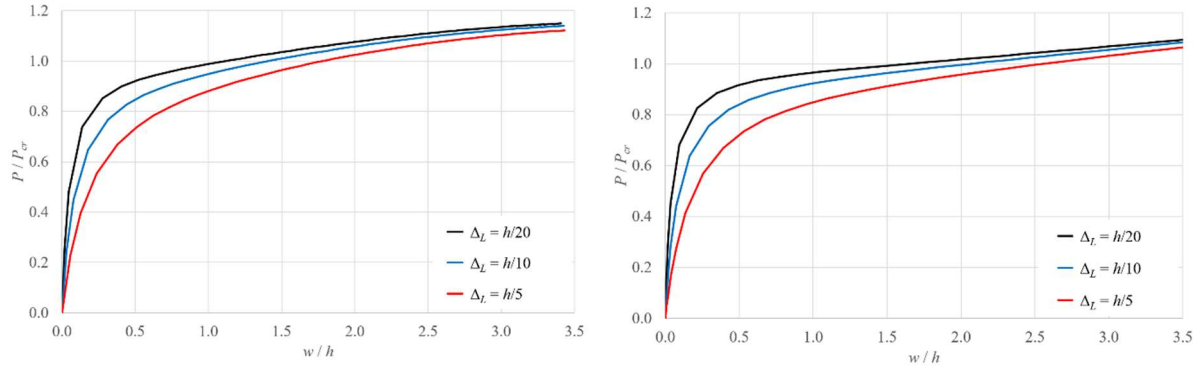
Layup	L (mm)	Δ_L (mm)			L (mm)	Δ_{FT} (mm)		
		$h/20$	$h/10$	$h/5$		$L/1500$	$L/1000$	$L/500$
L1	1000	0.0524	0.1048	0.2096	3000	2.0000	3.0000	6.0000
L2	500	0.0524	0.1048	0.2096	2000	1.3333	2.0000	4.0000

Additionally, the post-buckling behavior of the laminated columns was evaluated for cases involving pure buckling modes, without mode interaction. To capture the pure local post-buckling response, lengths of 1000 mm and 500 mm for the cross-ply and angle-ply columns, respectively (see Figure 1). To investigate the influence of the initial imperfections, the amplitudes considered were $\Delta_L = h/20$, $h/10$, and $h/5$. For the pure flexural-torsional global mode, the corresponding lengths were 3000 mm for the cross-ply column and 2000 mm for the angle-ply column, with initial imperfections amplitudes of $\Delta_{FT} = L/1500$, $L/1000$, and $L/500$. Table 3 presents the specific imperfection values used for each column.

3 Results and Discussion

This section presents and discusses the results regarding the influence of the initial geometric imperfection shape on the elastic post-buckling behavior of the two laminated channels defined in Section 2, focusing on their equilibrium paths, ultimate loads (when applicable), and collapse modes. For each column, post-buckling results associated with the initial imperfections introduced in the previous section are presented and discussed.

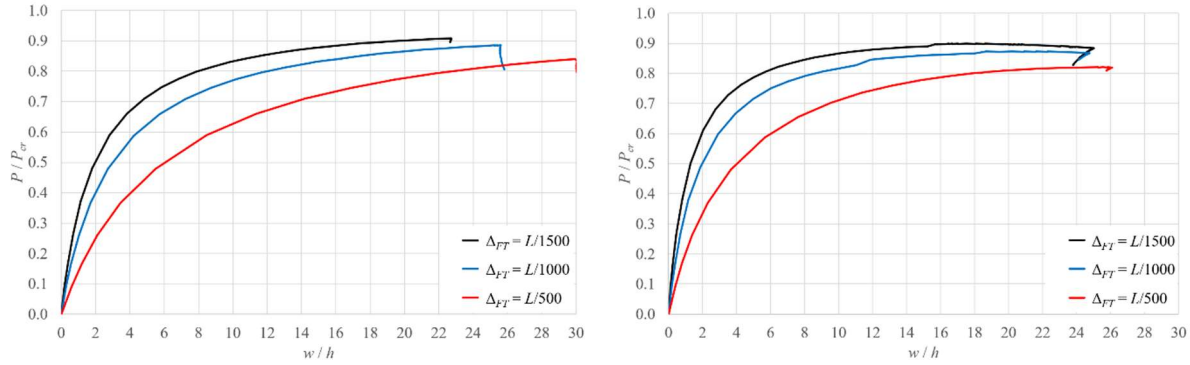
To illustrate these effects, the following figures present representative load-displacement curves for different buckling scenarios. Figure 2 and Figure 3 show the equilibrium paths obtained for the pure local and pure flexural-torsional buckling modes, respectively, based on the imperfections defined in Table 3, while Figure 6 displays the corresponding curves for the columns with transition-lengths between buckling modes, considering the initial imperfections combinations listed in Table 2. In all the figures, the maximum displacement w is measured at the free end of a flange, in the direction perpendicular to its undeformed position.



(a) Layup L1, with L = 1000 mm. (b) Layup L2, with L = 500 mm.

Figure 2. Load-displacement curves obtained for the pure local buckling mode.

In the case of short columns governed by local buckling (Figure 2), the structural response remains stable. As the initial imperfection amplitude increases, the columns exhibit greater flexibility, with larger transverse displacements under the same load level (behavior that is typical of plate-like structures). In contrast, columns undergoing flexural-torsional buckling (Figure 3) exhibit unstable behavior, characterized by a distinct ultimate load that decreases with increasing imperfection amplitude. Regarding the influence of layup, the cross-ply column shows superior post-buckling stiffness in the local buckling regime, while in the flexural-torsional case, it achieves a higher ultimate load for the same imperfection level, despite the angle-ply column displaying greater initial stiffness for small deformations (see Table 4). Figure 4 shows the deformed shapes of the columns governed by local buckling at the critical load, considering $\Delta_L = h/10$, while Figure 5 presents those affected by flexural-torsional effects at the ultimate load, with $\Delta_{FT} = L/1000$.

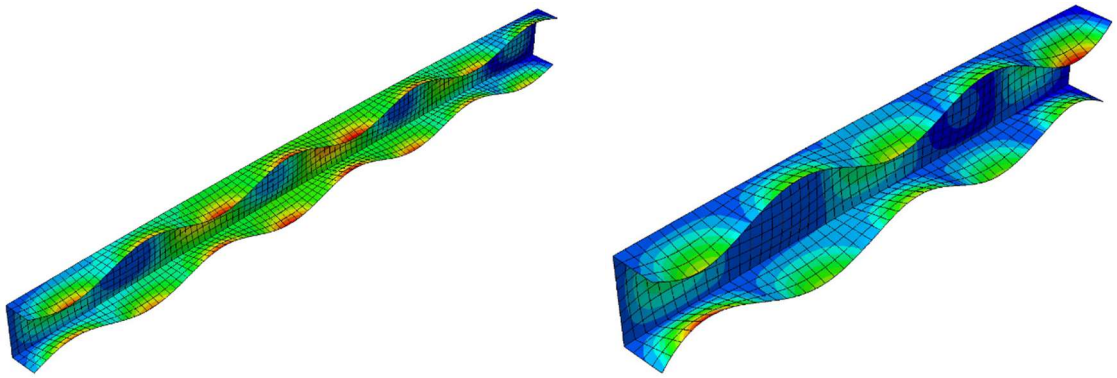


(a) Layup L1, with L = 3000 mm. (b) Layup L2, with L = 2000 mm.

Figure 3. Load-displacement curves obtained for the pure flexural-torsional buckling mode.

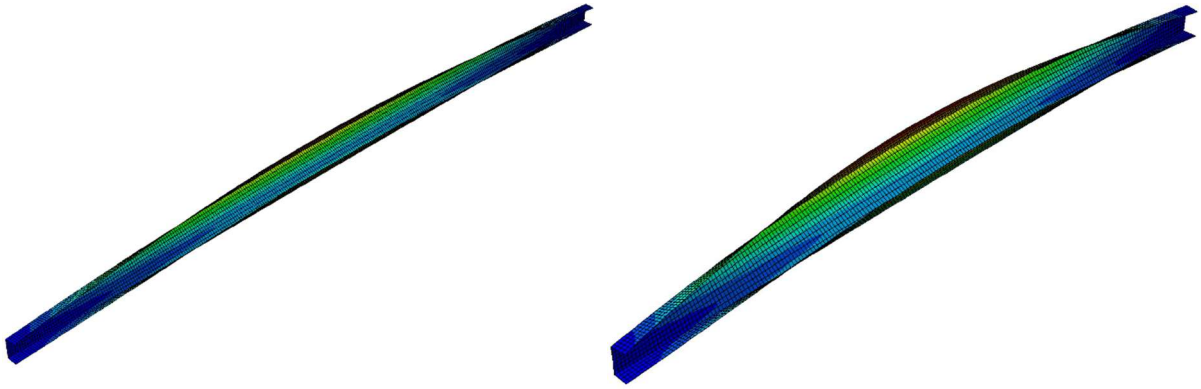
Table 4. Normalized ultimate load (P_u/P_{cr}) of the columns for the flexural-torsional buckling mode.

Layup	Δ_{FT}		
	L/1500	L/1000	L/500
L1	0.9082	0.8859	0.8404
L2	0.8986	0.8735	0.8202



(a) Layup L1, with L = 1000 mm. (b) Layup L2, with L = 500 mm.

Figure 4. Deformed shapes of the columns governed by local buckling at the critical load

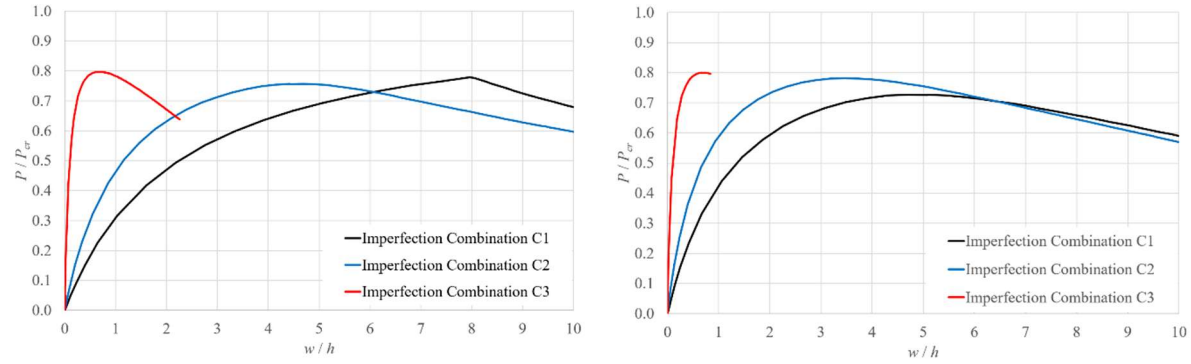


(a) Layup L1, with L = 3000 mm. (b) Layup L2, with L = 2000 mm.

Figure 5. Deformed shapes of the columns with flexural-torsional imperfections at the ultimate load.

Regarding the equilibrium paths obtained for the columns subjected to mode interaction, the structural response is also unstable, likely due to the influence of flexural-torsional effects. The ultimate loads for each case

are provided in Table 5. It is observed that the displacements resulting from purely local imperfections are significantly smaller than those associated with imperfections involving flexural-torsional components. Among the imperfection combinations evaluated, the greatest reduction in critical load for the cross-ply column was observed in combination C2, which resulted in a 24.3% decrease in load-carrying capacity, while for the angle-ply column, the most unfavorable case corresponded to combination C1, with a 27.3% reduction (see Table 5). Figure 7 shows the deformed shapes of the columns at the ultimate load.

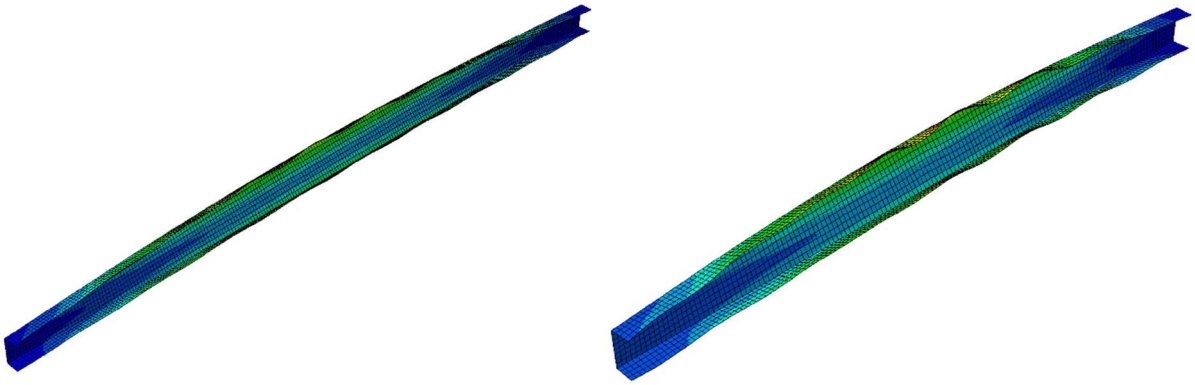


(a) Layup L1, with L = 2300 mm. (b) Layup L2, with L = 1460 mm.

Figure 6. Load-displacement curves obtained for the buckling modes transition lengths.

Table 5. Normalized ultimate load of the columns for each imperfection combination.

Imperfection Combination	P_u / P_{cr}	
	Layup L1	**Layup L2**
C1	0.7787	**0.7272**
C2	**0.7573**	0.7814
C3	0.7978	0.7996



(a) Layup L1, with L = 2300 mm. (b) Layup L2, with L = 1460 mm.

Figure 7. Deformed shapes of the columns for C2 imperfection combination at the ultimate load.

4 Conclusion

This study presented a sensitivity analysis to evaluate the influence of initial geometric imperfection shapes on the post-buckling behavior of simply supported laminated composite channel columns undergoing local-global interaction. The column lengths were selected based on the ratio $R = P_{cr,L}/P_{cr,FT}$, using a Rayleigh-Ritz approximation to estimate critical loads and construct signature curves. Finite element analyses were subsequently performed to refine the transition length estimates with greater accuracy. Nonlinear analyses were carried out for columns under both pure and interactive buckling conditions, with varied imperfection combinations to identify

the most critical scenarios for structural stability.

It was found that short columns governed by local buckling exhibit stable post-buckling behavior, whereas columns subjected to flexural-torsional or interactive buckling present unstable responses. The cross-ply column demonstrated higher post-buckling stiffness and greater ultimate load capacity in both regimes. Among the imperfection shapes evaluated, the combination between a flexural-torsional mode and a local mode led to the most significant reduction in critical load for the cross-ply column. For the angle-ply column the worst-case scenario was the flexural-torsional mode alone.

It is important to note that this is an ongoing study, and further investigations are required considering additional layups, geometric configurations, and support conditions, to draw more comprehensive conclusions. Future work will focus on identifying the range of $R = P_{cr,L} / P_{cr,FT}$ values for which modal interaction becomes significant in the equilibrium paths of the columns. Moreover, a more extensive evaluation of imperfection mode combinations is necessary to identify the most critical scenarios for the design of laminated columns.

Acknowledgements. The financial support by CNPq (Conselho Nacional de Desenvolvimento Científico e Tecnológico) and FUNCAP (Fundação Cearense de Apoio ao Desenvolvimento Científico e Tecnológico) are gratefully acknowledged.

Authorship statement. The authors hereby confirm that they are the sole liable people responsible for the authorship of this work and that all material that has been herein included as part of the present paper is either the property or authorship of the authors.

References

[1] S. Wang, T. Zhou, T. Liao, Y. Wang, L. Sang, L. Zhang. Local-global interaction buckling and load carrying capacity calculation method of cold-formed steel built-up closed section column. *Structures*, v. 71, pp. 107970, 2025.
[2] P. B. Dinis, D. Camotim, A. Landesmann, A. D. Martins, E. Cerqueira. Global–global interaction in cold-formed steel plain and lipped channel columns. *Thin-Walled Structures*, v. 172, 108872, 2022.
[3] E. Cerqueira, A. Landesmann, D. Camotim, P. B. Dinis, A. D. Martins. Direct strength prediction of cold-formed steel fixed-ended singly-symmetric columns buckling in flexural–torsional modes. *Thin-Walled Structures*, v. 187, 110730, 2023.
[4] E. J. Barbero. *Introduction to composite materials design*. CRC Press, 2011.
[5] J. N. Reddy. *Mechanics of laminated composite plates and shells: theory and analysis*. CRC Press, 2004.
[6] P. Czapski, A. J. G. Lunt. The influence of manufacturing on the buckling performance of thin-walled, channel-section CFRP profiles – an experimental and numerical study. *Thin-Walled Structures*, v. 184, 110475, 2023.
[7] H. Debski, T. Kubiak and A. Teter. Experimental investigation of channel-section composite profiles behavior with various sequences of plies subjected to static compression. *Thin-Walled Structures*, v. 71, pp. 147-154, 2013.
[8] H. Debski, A. Teter., T. Kubiak, S. Samborski. Local buckling, post-buckling and collapse of thin-walled channel section composite columns subjected to quasi-static compression. Composite Structures, v. 136, pp. 593-601, 2016.
[9] H. Debski, P. Rozylo, P. Wysmulski, K. Falkowicz, M. Ferdynus. Experimental study on the effect of eccentric compressive load on the stability and load-carrying capacity of thin-walled composite profiles. Composites Part B: Engineering, v. 226, 109346, 2021.
[10] P. Rozylo, H. Debski. Failure study of compressed thin-walled composite columns with top-hat cross-section. Thin-Walled Structures, v. 180, 109869, 2022.
[11] S. C. M. D'Aguiar, E. Parente Junior. Local buckling and post-critical behavior of thin-walled composite channel section columns. *Latin American Journal of Solids and Structures*, vol. 15, 2018.
[12] P. S. B. Barros, L. A. T. Mororó, E. Parente Junior. *Local and distortional buckling of thin-walled laminated lipped channel columns*. Proceedings of the XLV Ibero-Latin-American Congress on Computational Methods in Engineering, Maceió, Brazil, 2024.
[13] L. P. Kollár and A. Pluzsik. Analysis of thin-walled composite beams with arbitrary layup. *Journal of Reinforced Plastics and Composites*, vol. 21, n. 16, pp. 1423–1465, 2002.
[14] A. Pluzsik, L. P. Kollár. Effects of Shear Deformation and Restrained Warping on the Displacements of Composite Beams. *Journal of Reinforced Plastics and Composites*, vol. 21, n. 17, pp. 1517–1541, 2002
[15] P. S. B. Barros, L. A. T. Mororó, E. Parente Junior. *Global buckling of thin-walled composite columns with channel sections*. Proceedings of the 7th Brazilian Conference on Composite Materials, Brasília, Brazil, 2024.
[16] M. F. Pinto, P. S. B. Barros, L. A. T. Mororó, E. Parente Junior. *Evaluation of mechanical properties of laminated composite beams with open cross-sections*. Proceedings of the 7th Brazilian Conference on Composite Materials, Brasília, Brazil, 2024.
[17] R. Cook, D. Malkus, M. Plesha, R. J. Witt. *Concepts and applications of finite element analysis*. John Wiley & Sons, 2002.
[18] K. J. Bathe. *Finite element procedures*. Klaus-Jurgen Bathe, 1996.
[19] Simulia. *ABAQUS/Standard user's manual*. Version 6.13, Providence, RI, USA, 2013.